Environment. Technology. Resources. Rezekne, Latvia
Proceedings of the 16th International Scientific and Practical Conference. 2025. Volume IV, 169-180

Mechanical and Morphological Properties of PP/PE Composite Fishing Net Ropes

Inga Lasenko
Institute of Mechanical and Biomedical Engineering
Riga Technical University
Riga, Latvia
inga.lasenko@rtu.lv

Andris Martinovs
Engineering Centre, Rezekne Academy of Riga Technical University
Rezekne, Latvia
andris.martinovs@rta.lv

Artūrs Mačanovskis
Institute of Mechanical and Biomedical Engineering
Riga Technical University
Riga, Latvia
arturs.macanovskis@rtu.lv

Arta Viluma-Gudmona
Institute of Mechanical and Biomedical Engineering
Riga Technical University
Riga, Latvia
arta.viluma.gudmona@gmail.com

Sanjay Rajni Vejanand
Institute of Mechanical and Biomedical Engineering
Riga Technical University
Riga, Latvia
sanjay.vejanand@rtu.lv

Sandra Vasilevska
Faculty of Economics and Social Development
Latvia University of Life Sciences and Technologies
Jelgava, Latvia
sandra.vasilevsky@gmail.com

Sai Pavan Kanukuntla
Institute of Mechanical and Biomedical Engineering
Riga Technical University
Riga, Latvia
sai-pavan.kanukuntla@rtu.lv

***Abstract*— This study examined how the extrusion process, which is affected by different thermal settings, and the raw material sources, composed of various polypropylene (PP) and polyethylene (PE) blends with or without calcium carbonate ($CaCO_3$) additives, influence the quality and mechanical properties, such as tensile strength, elongation, and stiffness, of composite ropes for fishing net production. A comparative analysis of extrusion process parameters was conducted among four distinct extruders from the Promatech, Miyachi, Sima, and Ichikawa companies with a focus on their thermal settings, characterized by varying the temperature profiles. The investigation was extended to the utilization of PP derived from different sources and granule compositions, including formulations with $CaCO_3$ additives. In terms of breaking force, the samples with $CaCO_3$ showed an average increase of 5.2% when compared to those without $CaCO_3$. With the addition of $CaCO_3$, the elongation at break increased by an average of 8.7%. The addition of $CaCO_3$, surprisingly, resulted in a slight decrease in stiffness, averaging a decrease of 2.1% when compared to the samples without $CaCO_3$. Most significantly, the addition of $CaCO_3$ resulted in a significant decrease in Young's modulus, with an average reduction of approximately 66.4% compared to the samples without $CaCO_3$. This study reveals substantial differences in rope mechanical quality due to variations in raw materials and extrusion parameters, emphasizing the need for adapting the manufacturing process to consistently produce high-quality composite ropes for knitting fishing nets.**

Keywords*—Polypropylene; polyethylene; calcium carbonate additives; extrusion process parameters; composite ropes.

I. INTRODUCTION

Polymers have many applications in various industries, such as textiles [1], [2], packaging [3], automotive [4], aerospace [5], biomedical [6]–[9], and electronics [8], [10]. Some of the common properties of polymers are elasticity [11], [12], toughness, thermal stability, electrical conductivity, optical transparency, and biocompatibility [13], [14]. Composites are a type of materials that consists of a matrix material and reinforcing fibers [15]. Composite ropes are widely used for fishing net production, as they can withstand harsh marine environments and reduce the risk of ghost fishing [16]. Previous research indicates that approximately 2.5% of all fishing equipment is lost annually, encompassing over 78,000 km² of nets, more than 25 million pots and traps, and 740,000 km of longlines. The degradation of oceanic plastic debris, including discarded fishing gear, has significant implications for the health of

Online ISSN 2256-070X
https://doi.org/10.17770/etr2025vol4.8398

marine organisms and ecosystems. Marine plastics are hypothesized to serve as vectors for invasive species and pathogens across oceanic environments [17]. Among marine plastic debris, abandoned fishing nets, lines, and ropes are considered the most lethal forms, as they frequently result in the entanglement and subsequent mortality of various aquatic mammals, seabirds, and turtles [18].

The design and material choice of aquaculture nets can have a big impact on the industry's profitability, productivity, and environmental sustainability [19], [20]. The quality of these ropes is influenced by various factors, including the extrusion parameters during the manufacturing process and the characteristics of the raw materials used [21]. Among the different materials used for aquaculture nets, polypropylene (PP) and polyethylene (PE) are the most common and widely used synthetic polymers [22]. In terms of durability, strength, flexibility, buoyancy, UV resistance, and corrosion resistance, PP and PE outperform other materials such as nylon. PP and PE are also relatively inexpensive and simple to manufacture, making them suitable for aquaculture [23]. In particular, the choice of polypropylene (PP) as the primary material for composite ropes [24], as well as the potential inclusion of calcium carbonate ($CaCO_3$) additives, plays a significant role in determining composite ropes' mechanical properties and performance [25], [26].

$CaCO_3$ is specifically added to the granules with the objective of reducing stiffness and ensuring that the final ropes are flexible. This consideration holds particular significance in the context of weaving fishing nets, where flexibility is paramount, and rigid ropes present challenges during the fabrication process (fragile and high volume) [27]. By navigating the intricacies of variations in raw materials and $CaCO_3$ modifications, **this study aimed** to unravel the nuanced impact of these choices on the mechanical properties and suitability of composite ropes for specific applications.

Extrusion parameters, such as temperature settings, impact the structural integrity and flexibility of composite ropes. Different extrusion machines exhibit varying thermal profiles, which may result in variations in rope quality [28]. In this study, four different companies' extruders, Promatech, Miyachi, Sima, and Ichikawa, were compared in terms of their thermal settings.

Problem description: Comparative research has been conducted on the mechanical properties of composite ropes for fishing net production, particularly regarding the impact of extrusion process parameters and raw material variations. Previous studies have often focused on isolated factors, neglecting the complex interplay between extrusion conditions, polymer blends, and additives like $CaCO_3$. Moreover, the relationship between surface morphology and mechanical properties in these specialized composites remains poorly understood. This study aims to address these knowledge gaps by conducting a comprehensive analysis of the effects of diverse extrusion parameters and raw material compositions on the mechanical and surface properties of composite polymer ropes.

Despite theoretical expectations of a uniform rope quality, the existing empirical evidence suggests that differences in raw materials (polymers) and extrusion parameters lead to variations in rope thickness, bulk volume, and stiffness [29]. Currently, there is no standardized assessment on how raw materials and extrusion parameters may affect rope quality, which suggests that the manufacturing process can impact the quality of composite polymer ropes for knitting fishing nets in various ways. There are some standardized assessments for rope quality, such as ISO 9554:20191 [30], which specifies the general characteristics of fiber ropes and their constituent materials. Therefore, it is important to understand how the process parameters influence the quality of composite polymer ropes and ensure their consistency.

Limited comparative research has been conducted on the mechanical properties of composite ropes for fishing net production, particularly regarding the impact of extrusion process parameters and raw material variations. Previous studies have often focused on isolated factors, neglecting the complex interplay between extrusion conditions, polymer blends, and additives like $CaCO_3$. Moreover, the relationship between surface morphology and mechanical properties in these specialized composites remains poorly understood. This study aims to address these knowledge gaps by conducting a comprehensive analysis of the effects of diverse extrusion parameters and raw material compositions on the mechanical and surface properties of composite polymer ropes.

This study presents a comparative analysis of ten types of composite polymer ropes (with the same combination of polymer structures, as well as a variation of calcium carbonate), showing how the process parameters affect the quality of composite polymer ropes and how to adjust the manufacturing process to consistently produce high-quality composite ropes for knitting fishing nets. Understanding the intricate relationship between extrusion parameters and composite polymer raw materials is crucial in achieving the desired rope characteristics (physical and mechanical) and, ultimately, enhancing fishing net production.

II. Materials and Methods

A. Extruder Specifications and Thermal Settings

In this study, four distinct extruders, manufactured by different companies with the trade names Promatech, Miyachi, Sima, and Ichikawa (Table 1), were utilized to produce identical types of composite polymer ropes. Each extruder was characterized by specific thermal settings tailored to optimize both productivity and the quality of the resulting ropes. The thermal parameters for each extruder were meticulously controlled and varied.

TABLE 1 EXTRUDER SPECIFICATIONS

Extruder	Country	Screw Area Temperature (°C)	Outlet Temperature (°C)	Bath Temperature (°C)	Oven Temperature (°C)
Prometech	Italy	215-240	210	110	130
Miyachi	Japan	200-215	190	100	140
Sima	Italy	215-240	200	110	130
Ichikawa	Japan	205-220	205	110	140

B. Raw Material Selection and Utilization

The choice of raw materials influences the composition and characteristics of composite polymer ropes. The selection of distinct raw materials added complexity to the study, as variations in material properties could contribute to differences in the resulting composite ropes. This study strategically employed a diverse range of raw materials, consisting of polypropylene (PP) and polyethylene (PE). The PP was sourced from various companies, and included Capilene®, ©Rompetrol, Mosten® TB002, and Hyosung Topilene F501, each with distinct granules. Polyethylene (PE) granules were exclusively sourced from Orlen Unipetrol RPA (Czech Republic) Company (trademark: PE-HD Liten® TB 49-060) contributing to a standardized granule composition adopted across all ten manufactured ropes.

As described in the aforementioned references, adding $CaCO_3$ of different shapes and concentrations to polypropylene composites has been shown to enhance their mechanical properties. For instance, adding 10 wt% of homopolymer polypropylene (PP) with spherical $CaCO_3$ increased tensile and flexural strengths by 14.5% and 11.8%, respectively. Needle-like $CaCO_3$, at a 30 wt% concentration, resulted in a 20.6% increase in tensile strength and a 25.8% increase in flexural strength. Additionally, lower concentrations of $CaCO_3$, such as 5 wt%, demonstrated tensile and flexural strength enhancements of 12.7% and 8.9%, respectively. These variations highlight the importance of optimizing $CaCO_3$ content and shape to achieve specific mechanical performance targets in polypropylene composites. [31]–[34]. The masterbatch (granules) were composed of 70% polypropylene (PP) and 30% polyethylene (PE), with variations introduced in the 6th, 7th, 9th, and 10th samples through the addition of 5% and 10% $CaCO_3$, respectively (Table 2). The physical, mechanical, and thermal characteristics of the composite polymers utilized in this study are shown in Table 2.

The granule composition, a critical determinant of the mechanical and structural attributes, adhered to a consistent formulation—polypropylene (PP) (CAS Registry Number® 9003-07-0; molecular formula $(C_3H_6)_x$; melting point 158-170 °C; density 0.92 g/cm³) and polyethylene (PE) (CAS Registry Number® 9002-88-4; chemical formula: $(C_2H_4)_n$; flash point: 270 °C; density: 0.962 g/mL at 25 °C; melting point: 92 °C)—except for samples 6, 7, and 10. This deliberate blend sought to capture the synergistic effects of both polymers on the final properties of the composite polymer ropes. PP and PE were obtained from Sigma-Aldrich chemicals (Merck KGaA, Darmstadt, (64287) Germany).

$CaCO_3$ (calcium carbonate 99.95 Suprapur®, CAS 471-34-1, was obtained from Sigma-Aldrich chemicals (Merck KGaA, Darmstadt, (64287) Germany).

TABLE 2 COMPOSITION OF PP AND PE WITH/WITHOUT CACO3 ON EXTRUDER TYPE

No	Type of extruder	Polypropylene (PP) and concentration (%)	Polyethylene (PE) and concentration (%)	$CaCO_3$ (%)
1	Prometech extruder, Prometech Technologies, Crespellano—Bologna, Italy	PP Capilene® E 50 E, Polypropylene Homopolymer, Carmel Olefins Ltd (Israel) **70%**	PE-HD Liten® TB 49-060 Orlen Unipetrol RPA, (Czech Republic) **30%**	-
2	Prometech extruder, Prometech Technologies, Crespellano—Bologna, Italy	PP SS-05:F401 ©Rompetrol Refining SA, (Romania) **70%**	PE-HD Liten® TB 49-060 Orlen Unipetrol RPA, (Czech Republic) **30%**	-
3	Prometech extruder, Prometech Technologies, Crespellano—Bologna, Italy	PP Mosten® TB002, Unipetrol RPA, (Czech Republic) **70%**	PE-HD Liten® TB 49-060 Orlen Unipetrol RPA, (Czech Republic) **30%**	-
4	Miyachi extruder, Miyachi Iron Works, Ltd, Japan	PP Hyosung Topilene F501 (China) **70%**	PE-HD Liten® TB 49-060 Orlen Unipetrol RPA, (Czech Republic) **30%**	-
5	Sima extruder, Sima Headquarters, S.R.L., (MO) Italy	PP Mosten® TB002, Unipetrol RPA, (Czech Republic) **70%**	PE-HD Liten® TB 49-060 Orlen Unipetrol RPA, (Czech Republic) **30%**	-
6	Ichikawa extruder, Ichikawa Iron Works Co. Ltd, Japan	PP Capilene® E 50 E, Polypropylene Homopolymer, Carmel Olefins Ltd (Israel) **66.5%**	PE-HD Liten® TB 49-060 Orlen Unipetrol RPA, (Czech Republic) **28.5%**	5%
7	Ichikawa extruder, Ichikawa Iron Works Co. Ltd, Japan	PP Capilene® E 50 E, Polypropylene Homopolymer, Carmel Olefins Ltd (Israel) **63%**	PE-HD Liten® TB 49-060 Orlen Unipetrol RPA, (Czech Republic) **27%**	10%
8	Ichikawa extruder, Ichikawa Iron Works Co. Ltd, Japan	PP Capilene® E 50 E, Polypropylene Homopolymer, Carmel Olefins Ltd (Israel) **70%**	PE-HD Liten® TB 49-060 Orlen Unipetrol RPA, (Czech Republic) **30%**	-
9	Ichikawa extruder, Ichikawa Iron Works Co. Ltd, Japan	PP Capilene® E 50 E, Polypropylene Homopolymer, Carmel Olefins Ltd (Israel) **65%**	PE-HD Liten® TB 49-060 Orlen Unipetrol RPA, (Czech Republic) **30%**	5%
10	Ichikawa extruder, Ichikawa Iron Works Co. Ltd, Japan	PP Capilene® E 50 E, Polypropylene Homopolymer, Carmel Olefins Ltd (Israel) **70%**	PE-HD Liten® TB 49-060 Orlen Unipetrol RPA, (Czech Republic) **25%**	5%

TABLE 3 PHYSICAL, MECHANICAL, AND THERMAL CHARACTERISTICS OF POLYMER COMPONENTS

Polymer component	Capilene® E 50 E (PP)	SS-05: F401 (PP)	Mosten® TB 002 (PP)	Hyosung Topilene F501 (PP)	Liten® TB 49-060 (PE)
Melt Flow Rate (g/10 min)	1.8	2 - 3.5	2	3.0	0.6
Density (g/cm3)	0.905	0.905 - 0.917	0.902	0.90	0.949
Tensile Strength at Yield (MPa)	32	Min. 30	28	35.3	24
Flexural Modulus (MPa)	1400	Min. 900	1700	1570	1200
Izod Impact Strength (kJ/m2)	4	Min. 2	6.5	3.9	7
Vicat Softening Temperature (°C)	154	Min. 150	155	105	125
Heat deflection Temperature (°C)	96	Min. 45	55	150	80

C. Specimen Description

The commercially available ropes utilized in this study were manufactured using low-power, single-type extruders. Specifically, a one-screw extruders PP&PE FDY - 40 Tex, featuring 2 positions x 10 ends and a production capacity of up to 500 kg/hour, were employed. This equipment is operational at the SIA "MAGISTR" (24 Raina street, LV-5401, Daugavpils, Latvia) enterprise. The selection of this particular manufacturing process and supplier ensures consistency in the rope samples and aligns with industry standards for rope production (EN ISO 10572). Fig. 1 illustrates the comprehensive methodological process, beginning with rope material selection and culminating in comparative analysis (EN ISO 2062). This flowchart delineates the sequential steps of the procedure, providing a visual representation of the study's systematic approach.

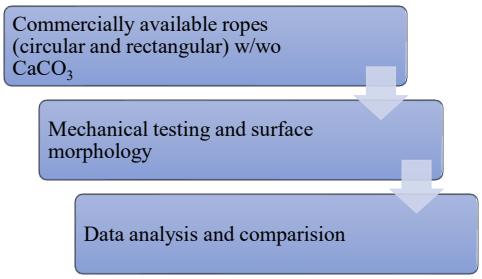

Fig. 1. Flowchart depicting the methodological sequence from initial rope selection to final comparative analysis.

The length of the specimens was measured using a Mitutoyo Strait-Line Tape Measure (Japan), which has a range of 0 – 3 m and two scales, one in metric and one in imperial units. The tape measure has a double coating at the end of the blade, a dual-sided hook, and a finger brake to control the retraction speed. The verification number is G366V22, 15.06.2023. The thickness of the specimens was determined using a Mitutoyo QuantuMike IP65 Digital Micrometer (Japan), which has a discreteness of 0.001 mm and a computer personal calibration at start-up. The digital micrometer has a coarser spindle thread that feeds the spindle by 2 mm per thimble revolution, a carbide measuring face, and a waterproof design. The mass of the specimens was determined using KERN PCB M Laboratory Scales (Germany), which have an accuracy class of II high, a maximum capacity of 200 g, and a discreteness of 0.01 g. The laboratory scales have a large LCD display, a stainless-steel weighing plate, and a shock-proof plastic housing. The calibration certificate number is M0901K22, 15.06.2023. The prepared specimens are shown in Fig. 2 in different shapes, such as circular and rectangular, and their parameters are summarized in Table 4. Figure 2(a) depicts the shape of samples 1–7 with a circular cross-section, whereas Fig2(b) depicts samples 8–10 with a rectangular cross-section.

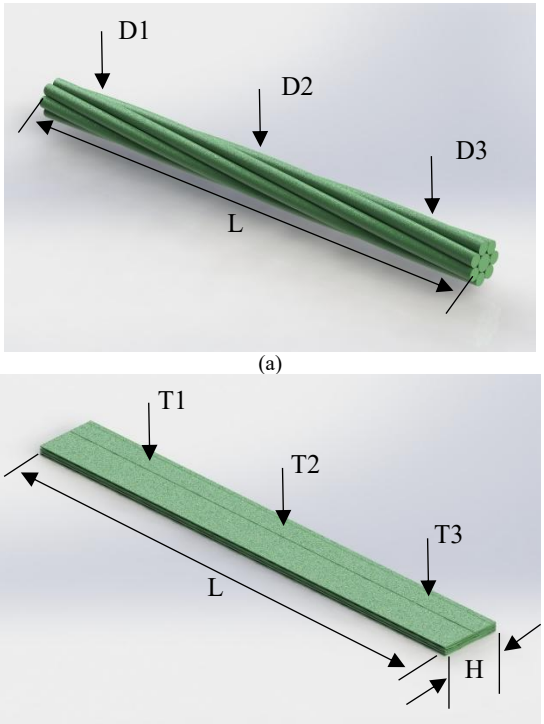

Figure 2. (a) Circular composite polymer rope and (b) rectangular composite polymer rope.

TABLE 4 SPECIMEN PARAMETERS

No.	Average Mass (g)	Initial Length (mm)	Average Thickness (mm)	Average Height (mm)	Average Diameter (mm)
1	0.1	100	-	-	0.416
2	0.103	100	-	-	0.432
3	0.110	100	-	-	0.443
4	0.1	100	-	-	0.420
5	0.11	100	-	-	0.405
6	0.105	100	-	-	0.407
7	0.1	100	-	-	0.401

8	0.031	100	0.353	1.241	-
9	0.034	100	0.430	1.240	-
10	0.032	100	0.294	1.221	-

D. Mechanical Testing: Breaking force and elongation at maximum breaking force

The samples were kept under normal conditions for 24 hours in a controlled environment according to the standard temperature, relative humidity, and pressure specified by ISO 139:19732. The breaking force and elongation at break of individual composite polymer rope specimens were measured using ISO 5079:2020. The physical and mechanical properties of the fiber ropes were measured using ISO 2307:2010. The process parameters for the standard atmospheres for conditioning and testing are shown in Table 5.

TABLE 5 PROCESS PARAMETERS FOR STANDARD ATMOSPHERES FOR CONDITIONING AND TESTING

Parameter	Value	Unit
Temperature	25±10; (21)	°C
Relative humidity	45-80; (W (% RM)) = 60	%
Atmospheric pressure	84.0-106.7; (760)	kPa (mm Hg)
Clamping length	10	cm
Clamping area	5	cm
Pre-load	5	H
Elongation speed	5	mm/s

E. Stiffness and Young's Modulus

The Young's modulus E (Pa) of the specimens was calculated using the following equation [35]:

$$E = \frac{FL}{A\Delta L} \quad \dots (1)$$

where F is the breaking force (N), L is the initial length (mm), A is the cross-sectional area (mm²), and ΔL is the elongation at maximum breaking force (mm). Young's modulus (E) is the material's stiffness and it measures the resistance to deformation under tensile stress [36].

The stiffness modulus k (N/m) of the specimens was calculated by multiplying the Young's modulus (E) by the cross-sectional area (A) and dividing by the initial sample length (L), as follows [35]:

$$k = EA/L \quad \dots (2)$$

The stiffness modulus k is the ratio of the applied force to the displacement caused by it along the same axis.

F. Study of the Samples' Surface Morphology

An Olympus LEXT OLS5000 3D Measuring Laser Microscope (Japan) was used to obtain surface images and 3D relief of the samples, and to measure their roughness. For this study, smooth areas on the sample surface without initial (113-1125 times magnification) visible defects—pores, cracks, or grooves—were selected at a magnification of 2255 times. This microscope allows us to obtain surface optical images and 3D models at 113, 227, 451, 1125, and 2255 times magnification for measuring the dimensions of the surface elements, and determining the surface roughness S_a (arithmetical mean height) (µm), S_z (maximum height) (µm), and S_q (root mean square height) (µm).

ISO 5079:2020

III. RESULTS AND DISCUSSION

A. Breaking force and elongation

The results shown in Table 6 indicate that the composite polymer ropes have different mechanical properties depending on the type. The highest average breaking force was observed for sample 3 (154.85 N), followed by sample 6 (149.11 N) and sample 5 (147.30 N). The lowest average breaking force was observed for sample 1 (73.04 N), followed by sample 4 (116.50 N) and sample 2 (122.12 N). The highest elongation at maximum breaking force was observed for sample 6 (13.28 mm), followed by sample 5 (12.76 mm) and sample 7 (12.20 mm). The lowest elongation at maximum breaking force was observed for sample 1 (5.51 mm), followed by sample 9 (9.99 mm) and sample 4 (8.61 mm). A visual comparative assessment of the test results of breaking force and elongation at maximum breaking force of the ten samples in accordance with ISO 5079:2020 is depicted in Fig. 3 and 4.

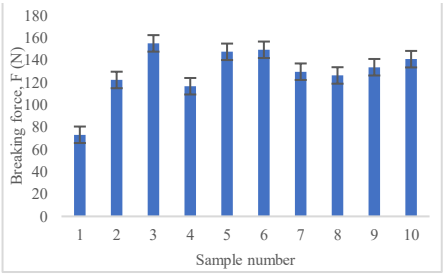

Fig. 3. Comparison graph of the values of breaking force of the ten samples

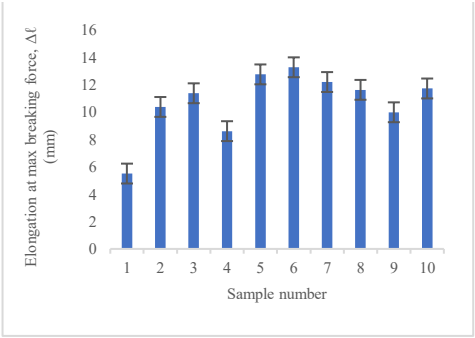

Fig. 4. Comparison graph of the values of elongation at maximum breaking force of the ten samples.

TABLE 6 TEST RESULTS OF BREAKING FORCE AND ELONGATION AT ISO 5079:2020 .KING FORCE

No.	Average Breaking Force, F (N)	Average Elongation at Max. Breaking Force, Δℓ (mm)
1	73.04	5.51
2	122.12	10.38
3	154.85	11.38
4	116.50	8.61
5	147.30	12.76
6	149.11	13.28
7	129.50	12.20

8	126.14	11.63
9	133.51	9.99
10	140.72	11.73

The samples processed through the Prematech and Sima extruders (samples 1, 3, 5, and 8) exhibited higher breaking forces, indicative of enhanced structural integrity. The elevated screw area temperatures and medium-to-hard rope hardness contributed to better molecular alignment and interfacial adhesion. In contrast, the samples processed with the Miyachi and Ichikawa extruders (samples 2, 4, 6, 7, 9, and 10) showed lower breaking forces, suggesting that lower screw area temperatures and softer rope hardness may lead to reduced tensile strength.

The breaking force of 73.05 N observed in sample 1, which was the lowest breaking force observed among all samples, produced by the Prematech extruder with the highest screw area temperature and medium rope hardness, aligns with the general trend. The highest breaking force of 154.85 N was observed in sample 3, which was composed of 30% PE-HD Liten® TB 49-060 and 70% PP Mosten® TB002. These results can be attributed to the specific combination of polymer blend composition and extrusion process parameters employed by both the Prematech and Sima extruders.

The $CaCO_3$ filler content also had a significant effect on the breaking force and elongation of the ropes. The ropes with 5% $CaCO_3$ filler (samples 9 and 10) had relatively a lower average elongation (compared to the sample 6) but samples 6 and 10 had higher breaking force compared to the sample 9. Sample 6, with 5% $CaCO_3$, displayed the highest breaking force (149.11 N) among all samples (excluding sample 3), emphasizing the positive impact of $CaCO_3$ in enhancing the mechanical properties. The average breaking force of the ropes with 5% $CaCO_3$ increased by 14.42 % (compared to the ropes without $CaCO_3$). The average elongation at break of the ropes with 5% $CaCO_3$ increased by 16.18% compared to the ropes without $CaCO_3$. This shows that the $CaCO_3$ filler enhanced the strength and stiffness of the ropes by acting as a reinforcing agent.

The rope with a higher 10% $CaCO_3$ filler content (sample 7) had on 1.34 time average elongation higher (than samples 9 and 10) but on 11.61 time lower breaking force than the ropes with a lower 5% $CaCO_3$ filler content (samples 6, 9 and 10). This shows that the 10% $CaCO_3$ filler (compared to 5% $CaCO_3$) reduced the strength and stiffness of the ropes by acting as a diluent, lowering the polymer content, as well as the interfacial adhesion and molecular orientation of the polymer chains, thereby leading to more flexible and weaker ropes.

B. Stiffness and Young's modulus

Table 7 represents the stiffness and Young's modulus results obtained from mechanical testing, where among all the results, the two best and the two lowest, close in value, were distinguished. The samples with the highest stiffness were observed for: sample 3 ($137.39*10^2$ N/m) and sample 4 (135.67*102 N/m), while the lowest stiffness were noted: for sample 7 ($106.12*10^2$ N/m) and sample 8 ($108.46*10^2$ N/m). Similarly, the highest Young's modulus were observed for: sample 1 (9.8 GPa) and sample 4 (9.725 GPa), and the lowest Young's modulus were observed for: sample 8 (2.478 GPa) and sample 9 (2.499 GPa). A visual comparative assessment of the calculative results of stiffness and Young's modulus in the ten samples in accordance with ISO 2307:2010 is depicted in Fig. 5 and 6.

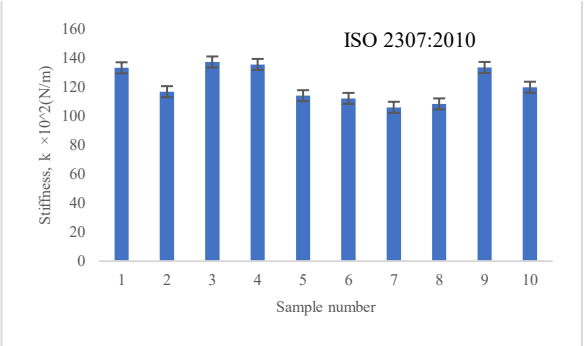

Fig. 5. Comparison graph of the stiffness values of the ten samples.

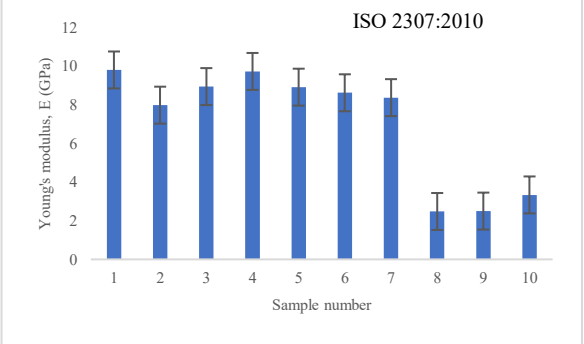

Fig. 6. Comparison graph of Young's modulus values of the ten samples.

TABLE 7. RESULTS OF STIFFNESS AND YOUNG'S MODULUS

No.	Stiffness, *k* (N/m)	Young's modulus, *E* (GPa)
1	$133.36*10^2$	9.8
2	$116.89*10^2$	7.98
3	$137.39*10^2$	8.94
4	$135.67*10^2$	9.725
5	$114.11*10^2$	8.91
6	$112.24*10^2$	8.62
7	$106.12*10^2$	8.369
8	$108.46*10^2$	2.478
9	$133.59*10^2$	2.499
10	$119.96*10^2$	3.335

The Prematech extruder, with a higher screw area temperature and medium rope hardness, resulted in sample 1 having the highest stiffness ($133.36*10^2$ N/m) and Young's modulus (9.8 GPa). The elevated temperatures likely facilitated better molecular alignment, leading to increased stiffness. This aligns with the general understanding that higher processing temperatures

contribute to a more ordered polymer structure [33], resulting in higher stiffness and Young's modulus.

Sample 3, utilizing Mosten® TB002, demonstrated the highest stiffness ($137.39*10^2$ N/m). The unique properties of Mosten® TB002, possibly related to molecular weight or chain architecture, contributed to the observed higher stiffness. This indicates the significance of raw material selection in achieving the adapted mechanical properties in polymer composite ropes.

The samples with higher stiffness and Young's modulus (samples 1, 3, and 4) were produced by the Promatech and Sima extruders, had a higher PP content, and did not have $CaCO_3$ filler. The samples with lower stiffness and Young's modulus (samples 7, 8, 9, and 10) were produced by the Miyachi and Ichikawa extruders, had a lower PP content, and had $CaCO_3$ filler. These results confirm that higher temperature and hardness of the extruders, higher PP content of the blends, and the absence of $CaCO_3$ filler enhanced the stiffness and Young's modulus of the ropes, while lower temperature and hardness of the extruders, lower PP content of the blends, and the presence of $CaCO_3$ filler reduced the stiffness and Young's modulus of the ropes. The obtained result well correlated with [37].

Samples 6, 7, and 9, containing $CaCO_3$, exhibited improved stiffness compared to their counterparts without $CaCO_3$. Sample 6, with 5% $CaCO_3$, demonstrated the highest stiffness ($112.24*10^2$ N/m), indicating that the addition of $CaCO_3$ contributed to the composite rope's stiffness. The positive impact of $CaCO_3$ on stiffness is in line with its role in reducing the overall rigidity of the composite rope, making it more flexible for specific applications. $CaCO_3$ addition, surprisingly, resulted in a modest reduction in stiffness, with $CaCO_3$-containing samples showing an average decrease of 2.1% compared to those without $CaCO_3$. $CaCO_3$ led to a significant reduction in Young's modulus, with the $CaCO_3$-containing samples showing an average reduction of approximately 66.4% compared to samples without $CaCO_3$.

The breaking force of the Ichikawa extruder-produced composite ropes surpassed those observed in prior studies by 51.49% to 54.07%, indicating a significant improvement in mechanical performance. Comparative analysis with prior studies [32], [38], and [39] reveals that sample 6 (66.5% PP, 28.5% PE, 5% $CaCO_3$) exhibits a 54.07% higher breaking force than that reported in a prior study [32] (70% PP, 25% PE, 5% $CaCO_3$). This improvement is attributed to sample 6's higher PP content and lower PE content, enhancing its stiffness, strength, and crystallinity, while a lower $CaCO_3$ content reduces brittleness and stiffness, and improves ductility and impact resistance. Similarly, the elongation at maximum breaking force surpasses that observed in prior studies by 51.85% to 56.32%. Notably, sample 6 displays a 56.32% higher elongation compared to study [32], credited to its lower PP content and higher PE content, thereby promoting its ductility, toughness, and flexibility. Maintaining the same $CaCO_3$ content as study [38] minimized the impact on composite deformation and strain. In contrast, stiffness was 17.04% to 21.88% lower compared with studies [32], [38], and [39]. Specifically, sample 9 (65% PP, 30% PE, 5% $CaCO_3$) exhibited a 21.88% higher stiffness than a prior study [38], attributed to its higher PE and lower $CaCO_3$ content, improving ductility and flexibility. A lower PP content reduced the modulus, strength, and crystallinity, enhancing deformation and strain. Also, it should be noted, Young's modulus was 9.05% to 12.45% lower, with sample 9 displaying a reduction of 12.45% compared to study [40]. This is attributed to sample 9's higher PE and lower $CaCO_3$ content, reducing stiffness, strength, and crystallinity, along with a lower PP content further reducing the modulus and improving deformation and strain.

Lastly, at 5 wt% $CaCO_3$, it is well dispersed in the matrix. However, at a higher ratio, the $CaCO_3$ particle (compared with 10 wt%) tends to gather to form bigger clusters; therefore, these clusters could play as defects, resulting in lower mechanical properties. The interfacial connection and compatibility between PE, PP, and $CaCO_3$ reinforce the mechanical properties of the plastic. This effect could be mostly generated from the formation of β-form crystalline of PP, caused by the synergistic effect between PE and $CaCO_3$ [41], [42].

C. Study of the Surface Morphology of the Samples

Fig. 7 shows the surface structure of the sample 1. These are presented under two different magnifications: (a) 113 times (image area size of 2.57 x 2.57 mkm) and (b) 2255 times (image area size of 128 x 127 mkm). The red squares in (a) show the corresponding location in (b) under higher magnification. The colored scale in (b) shows the height change in mkm on the viewed surface. The measurement of surface roughness was carried out along 30 points on the sample surface (along the transverse line based on the mode indicated in Fig. 7), and the average value is shown in Table 8.

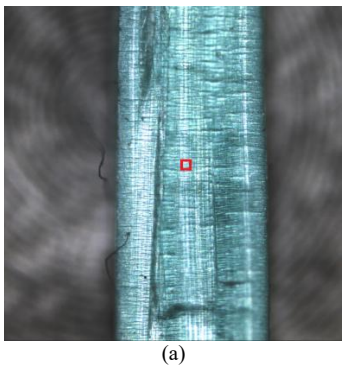

(a)

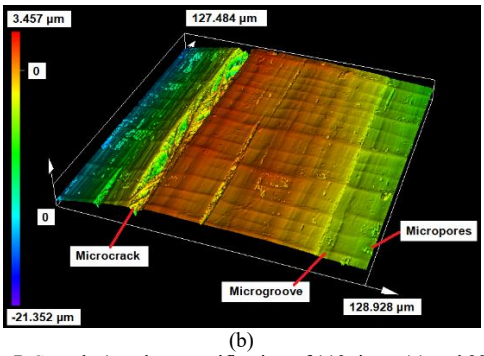

(b)

Fig. 7. Sample 1 under magnification of 113 times (a) and 2255 times (b).

In samples 1 and 4–10, in the longitudinal direction of the fiber, microgrooves can be observed on the surface (in samples 1, 6, and 7, there are possibly also microcracks because they have an uneven surface), with a width and depth of 1–8 µm; in samples 2 and 3, there are practically no microgrooves.

In samples 1–5, in the transverse direction of the fiber, there are ridges (ramps) that are 0.5–2.5 µm high (the surface of all these ridges is smooth); in samples 6–10, there are practically no such ridges.

The surface roughness was measured in a square size of 32 x 32 µm located in the center of the analyzed area (128 x 127 µm) of the sample (Fig. 8). A relatively small area (32 x 32 µm) was used because the surface of the samples is not flat (it is curved). In this case, only the microstructure was studied (the macrostructure with its defects was not taken into account). Surface roughness S_a, S_z, and S_q are shown in Table 8.

The surface of sample 3 has the least number of defects and one of the smallest roughness values. Perhaps for this reason, the breaking force (Table 6) and stiffness (Table 7) are the highest for this sample in comparison with the other nine samples.

It is highly important to know and analyze the surface morphology of a material, primarily due to the performance characteristics of the product (the fishing net).Microscopic abrasive particles (sand, corundum, etc.), which are present in seawater, can become stuck on surface defects (micropores, microgrooves, and microcracks) [43]. During operation, they will accelerate the material's wear process. Additionally, seawater is an "aggressive" environment for the operation of rope materials due to the seawater chemical composition. Six major ions make up > 99% of the salts dissolved in seawater: four cations—sodium (Na^+), magnesium (Mg^{2+}), calcium (Ca^{2+}), and potassium (K^+)—and two anions—chloride (Cl^-) and sulfate (SO_4^{2-}) [44]. These six ions and the five next most common ones make up the major constituents of seawater and comprise 99.99% of dissolved materials; they have a chemical effect on rope materials and accelerate their aging; this leads to the breakdown of the polymer chains (in materials made of polymer fiber) [45]. Aging is faster on surface defects. Both wear and aging processes reduce the lifespan of fishing nets. Therefore, a material with a minimum number of surface defects is optimal. In this investigation, it is sample number 3.

In the comparison of surface values, samples 1, 2, 4, 6, 7, 9, and 10 exhibit moderate surface roughness, indicating a textured surface. The variations observed can be attributed to differences in extruder types, polymer compositions, and the inclusion of $CaCO_3$. In particular, sample 8 deviates from the trend with a higher surface roughness value of 0.324±0.071 µm (S_a). However, it is crucial to note that this result comes with a relative error, emphasizing the necessity of considering measurement uncertainties during surface roughness assessments.

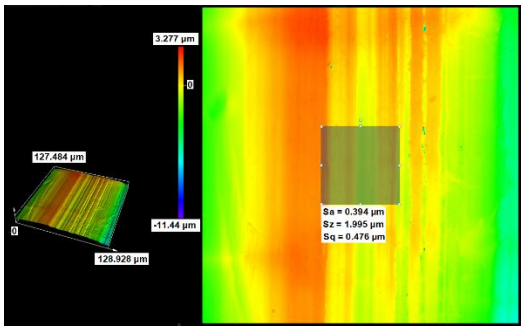

Fig. 8. Example of roughness measurement (sample no. 8).

TABLE 8. RESULTS OF SURFACE ROUGHNESS

No.	Average Roughness Sa (µm)	Average Roughness Sz (µm)	Average Roughness Sq (µm)
1	0.282	6.273	0.366
2	0.227	3.228	0.303
3	0.178	1.104	0.215
4	0.206	4.081	0.318
5	0.228	3.180	0.316
6	0.233	2.592	0.280
7	0.284	2.997	0.361
8	0.324	2.042	0.383
9	0.145	5.905	0.231
10	0.165	4.555	0.206

The relative errors of each measurement were S_a=22%, S_z=20%, and S_q=23%.

The roughness of the rope material may have a positive effect on the adhesion of the fibers in the rope, depending on the type of material, the type of extruder, and the type of additive [46]. Roughness can increase the surface area and the mechanical interlocking of the fibers, which can improve the cohesion and strength of the rope [47]. However, roughness can also introduce defects and irregularities that can reduce the uniformity and quality of the rope [48]. Therefore, the optimal roughness of the rope material depends on the balance between these factors. According to a study conducted at the University of Pittsburgh, surface roughness affects the functional properties of surfaces, including adhesion [49]. Roughness imparts an additional surface area with which an adhesive can make contact when forming a bond. Another study found that there is a clear dependency between the adhesive bond strength and surface roughness [50].

Roughness, micropores, and microcracks primarily affect the strength characteristics (strength and reliability of the sample).

For the first sample, the average roughness index (S_z) is 6.273 μm and the number of micropores (in the study area) is the highest compared to the other nine samples. Therefore, the breaking force (F_1=73.04±2 N) is almost two times lower than that for the other nine samples. However, it is possible the high surface roughness of the filaments (S_a = 0.282±14 mkm, S_z = 6.273±13 mkm, and S_q = 0.366±12 mkm), in combination with the physical and mechanical properties of the composite polymer (PP, PE) (Table 2), has an impact on the stiffness value of the sample, which shows one of the highest values of k_1=133.36*10^2 N/m in comparison to samples 2, 5, 6, 7, 8, and 10 (the average value of which is k_{avg}=112*10^2 N/m). At the same time, Young's modulus (which determines the properties of the material) is also the highest (E_1=9.8 GPa) out of the 10 samples studied. With a slight deviation, the same values of Young's modulus are characteristic of samples 2–7 (Table 5); their values are almost 3.3 times higher than those for samples 8–10.

It is possible that the roughness and strength of a material are influenced by its production conditions (the technical data for the production of the samples on an extruder). For example, with the same combinations of composite materials (comparing the first and eighth samples) but produced on different types of extruders (first sample—Promatech extruder; eighth sample—Ichikawa extruder; Table 1), the breaking force for the eighth sample is 1.73 times higher than that for the first sample, while the roughness (compared using the S_z value) is three times less. It can also be noted that using composite raw materials from different suppliers (for example, first sample: PP Capilene®, PE-HD Liten®; second sample: PP SS-05:F401, PE-HD Liten®; third sample: PP Mosten® TB002, PE-HD Liten® (Table 1)), but with the samples produced on the same type of equipment (Promatech extruder), results in different values of the breaking force, namely, the breaking force increases algebraically (F_1=73.04±2 N; F_2=122.12±2 N; F_3=154.85±3 N), and the elongation at break $\Delta\ell$ increases accordingly (Table 4). This means that under the same production conditions (on the same type of extruder equipment), but using different types of raw materials, we obtain different values for the physical and mechanical parameters of the samples [32], [37], [51].

However, when comparing the stiffness and Young's modulus for samples 1–3, it can be noted that the stiffness of the second sample is significantly lower (k_2=116.89*10^2 N/m) than the average value for the first and third samples (k_{avg}=135.38 *10^2 N/ m). The same pattern is observed for the Young's modulus values (E_2 = 7.98 GPa; for the first and third samples: E_1 = 9.8 GPa and E_3 = 8.94 GPa). Furthermore, during the tactile subjective assessment, it was noted that the second sample was the hardest to the touch compared to the other nine samples. This means that the production of the final products (such as fishing nets) will be significantly difficult (in the process of knitting fibers on textile machines).

The same pattern (during tactile assessment) was observed for the fifth sample (the sample was hard to the touch). The values of roughness, stiffness, and Young's modulus, when compared with the corresponding values for the second and fifth samples, are correlated. However, the values of breaking force and elongation at maximum breaking force of the fifth sample (F_5=147.30±3 N; $\Delta\ell_5$=12.76±0.4 mm) are higher than those for the second sample (F_2=122.12±2 N; $\Delta\ell_2$=10.38±0.2 mm) (Table 4). Obviously, the quality indicators of the fifth sample are influenced by either the type of raw materials (PP Mosten® TB002; PE-HD Liten®) or the type of extruder equipment selected (technological production conditions) (Sima extruder) (Table 1).

Regarding tactile properties, it can be noted that the fourth sample is characterized by high softness compared to the other nine samples. Despite this, the fourth sample is characterized by high stiffness values (k_5=135.67*10^2 N/m) and Young's modulus (E_5=9.725 GPa), compared to the corresponding values for samples 2, 5, 6, 7, 8, and 10, whose average values are k_{avr}=112.96*10^2 N/m and E_{avr}=6.62 GPa (Table 5). However, the average roughness value, which is almost two times higher than that for samples 3, 6, 7, and 8, and the presence of microcracks affect the breaking force (F_4=116.50±1 N) and elongation of the sample ($\Delta\ell_4$=8.61±0.3 mm), whose values are the lowest compared to the other samples (3, 5, 6, 7, 8, 9, and 10).

The inclusion of $CaCO_3$ in the composition of the polymer material (sixth and seventh samples, Table 1) did not affect the roughness indicators of the samples, compared to the eighth sample (without $CaCO_3$). However, the addition of $CaCO_3$ affected the presence of longitudinal microcracks in the sixth and seventh samples. This may be a consequence of insufficient homogeneity of the polymer composite. It should be noted that the addition of $CaCO_3$ to the composition of the polymer (sixth sample) sharply increased the breaking force F_6=149.11±4 N and elongation at maximum breaking force $\Delta\ell_6$=13.28±0.3 mm, compared with the values of the breaking force and elongation at maximum breaking force of the seventh and eight samples: F_7=129.50±2 N; $\Delta\ell_7$=12.20±0.2 mm; F_8=126.14±3 N; $\Delta\ell_8$=11.63±0.4 mm. However, the stiffness values for samples 6, 7, and 8 practically correlate, with k_{avr}=108.94*10^2 N/m, but the value of Young's modulus for the eighth sample (without $CaCO_3$) is 3.4 times lower than for that of the sixth and seventh samples. This proves that the presence of $CaCO_3$ in the composite increases the breaking force, elongation at maximum breaking, stiffness, and elastic modulus, and 5% $CaCO_3$ is preferable to 10% $CaCO_3$, it correlates with [31].

Adding 5% of $CaCO_3$ to the composition of the polymer material in such a way that the percentile amount of either PP or PE is changed (ninth and tenth samples, Table 1) leads to a significant increase in the sample surface roughness (S_z) by almost 2.5 times compared to the

roughness values for samples 6, 7, and 8 (samples 6–10 were produced on the same type of Ichikawa extruder and the same types of raw materials were used), which allows us to compare the roughness values and physical and mechanical characteristics with each other. As shown in the analysis of the surface structure of the ninth and tenth samples, they are characterized by micropores. This may also be the result of insufficient homogenization of the polymers, combined with the addition of 5% $CaCO_3$ to the composite structure. However, with such a percentage combination of PP, PE, and 5% $CaCO_3$ (ninth and tenth samples), the values of the breaking force increase significantly and amount to F_9=133.51±2 N and F_{10}=140.72±3 N compared with the values of the breaking force for samples 6, 7, and 8. There is also an increase in the stiffness of the ninth and tenth samples: k_9=133.59*10^2 N/m and k_{10}=119.96*10^2 N/m compared to samples 6–8, whose average value is k_{avr}=108.94*10^2 N/m. At the same time, the Young's modulus, which characterizes the ability of a material to resist tension, during the elastic deformation of the ninth sample is E_9=2.449 GPa; for the tenth sample, it increases slightly to E_{10}=3.335 GPa.

However, the average value of Young's modulus for the ninth and tenth samples correlates with the value of Young's modulus for the eighth sample (without $CaCO_3$) but is three times lower than for the sixth and seventh samples (E_{avr}=8.49 GPa). If we optimize the choice of the combination of polymer components in the composite based on the breaking force (between the ninth and tenth samples), and then with the percentage of components for the tenth sample (PP 70%; PE 25%; $CaCO_3$ 5%), the breaking force is higher than for the ninth sample. However, the surface roughness of the ninth and tenth samples (when comparing their values with samples 6, 7, and 8) is two times higher; this negatively affects the performance characteristics of products such as fishing nets.

These findings have significant implications for the fishing industry and other sec-tors utilizing composite polymer ropes. By optimizing extrusion parameters, carefully se-lecting raw materials, and judiciously incorporating additives like $CaCO_3$, manufacturers can tailor rope properties to meet specific application requirements. This level of custom-ization could lead to improved performance, longevity, and sustainability of fishing gear and other rope-based products.

Future research directions may include further investigation into the long-term per-formance and durability of composite ropes under various environmental conditions, the exploration of additional additives or surface treatments to enhance specific properties such as UV resistance or biodegradability, and the development of predictive models to streamline the optimization process for new composite rope formulations.

IV. CONCLUSIONS

This study demonstrates that the mechanical properties of composite polymer ropes result from a complex interplay between extrusion process parameters, polymer composition, and the inclusion of calcium carbonate ($CaCO_3$).

The choice of the extruder and its associated parameters proved crucial in determining the rope quality. Notably, the Promatech and Sima extruders, characterized by higher (11.6-17.1%) screw area temperatures and medium-to-hard rope hardness, generally produced ropes with superior breaking forces. These findings highlight the importance of optimizing the processing conditions to achieve the desired mechanical properties in composite ropes.

The incorporation of $CaCO_3$ yielded positive results in terms of flexibility enhancement. The samples containing $CaCO_3$ exhibited an average increase of 14.42% in breakingforce compared to those without, indicating a reinforcement effect that contributed to increased flexibility and energy absorption capacity. However, this study also revealed an optimal $CaCO_3$ content of 5%, beyond which mechanical properties may begin to deteriorate, suggesting a threshold effect for $CaCO_3$ reinforcement.

The selection of raw materials emerged as a significant factor influencing rope properties. The use of Mosten® TB002 in sample 3 resulted in exceptional breaking force (154.85 N) and stiffness (137.39*10^2 N/m), demonstrating the potential for tailoring rope properties through the careful selection of polymer blends.

An analysis of the surface morphology revealed a correlation between surface defects, roughness, and mechanical properties. Sample 3, with the lowest number of surface defects and one of the lowest roughness values, exhibited the highest breaking force and stiffness (137.39*10^2 N/m) among all samples. This finding emphasizes the importance of surface quality in determining the overall performance of composite ropes and suggests that minimizing surface defects could be a key strategy for enhancing rope durability and strength.

This research elucidated important relationships between processing conditions, structural characteristics, and the final properties of composite ropes. These processing–structure–property relationships provide valuable insights for optimizing production processes to achieve the desired rope characteristics.

ACKNOWLEDGEMENT

This work has been supported by research and development grant No RTU-PA-2024/1-0091 under the EU Recovery and Resilience Facility funded project No. 5.2.1.1.i.0/2/24/I/CFLA/003 "Implementation of consolidation and management changes at Riga Technical University, Liepaja University, Rezekne Academy of Technology, Latvian Maritime Academy and Liepaja Maritime College for the progress towards excellence in higher education, science, and innovation"

REFERENCES

[1] B. Baye and T. Tesfaye, "The new generation fibers: a review of high performance and specialty fibers," Polym. Bull., vol. 79, no. 11, pp. 9221–9235, 2022, doi: 10.1007/s00289-021-03966-6.

[2] I. Lasenko, J. V Sanchaniya, S. P. Kanukuntla, A. Viluma-Gudmona, S. Vasilevska, and S. R. Vejanand, "Assessment of Physical and Mechanical Parameters of Spun-Bond Nonwoven Fabric," Polymers, vol. 16, no. 20. 2024. doi: 10.3390/polym16202920.

[3] K. Dharmalingam and R. Anandalakshmi, Polysaccharide-Based Films for Food Packaging Applications. 2019. doi: 10.1007/978-981-32-9804-0_9.

[4] H. Mohammadi, Z. Ahmad, S.A. Mazlan, M.A. Faizal Johari, G. Siebert, M. Petrů, S.S. Rahimian Koloor, "Lightweight Glass Fiber-Reinforced Polymer Composite for Automotive Bumper Applications: A Review," Polymers (Basel)., vol. 15, no. 1, pp. 1–30, 2023, doi: 10.3390/polym15010193.

[5] V. T. Rathod, J. S. Kumar, and A. Jain, "Polymer and ceramic nanocomposites for aerospace applications," Appl. Nanosci., vol. 7, no. 8, pp. 519–548, 2017, doi: 10.1007/s13204-017-0592-9.

[6] J. Jeevanandam, S. Pan, J. Rodrigues, M. A. Elkodous, and M. K. Danquah, "Medical applications of biopolymer nanofibers," Biomater. Sci., vol. 10, no. 15, pp. 4107–4118, 2022, doi: 10.1039/D2BM00701K.

[7] J.V. Sanchaniya, I. Lasenko, S.-P. Kanukuntala, H. Smogor, A. Viluma-Gudmona, A. Krasnikovs, V. Gobins, I. Tipans, "Mechanical and thermal characteristics of annealed-oriented PAN nanofibers," Polymers (Basel)., 2023, doi: doi.org/10.3390/polym15153287.

[8] J. V. Sanchaniya, I. Lasenko, S. P. Kanukuntla, A. Mannodi, A. Viluma-gudmona, and V. Gobins, "Preparation and Characterization of Non-Crimping Laminated Textile Composites Reinforced with Electrospun Nanofibers," Nanomaterials, vol. 13, no. 13, p. 1949, 2023, doi: 10.3390/nano13131949.

[9] D. Grauda, D. Butkauskas, R Vyšniauskienė, V. Rančelienė, N. Krasņevska, A. Miķelsone, K. Žagata, V. Gobiņš, I. Rashal, D. Rašals,, "Establishment of Biotesting System to Study Features of Innovative Multifunctional Biotextile," Proc. Latv. Acad. Sci. Sect. B Nat. Exact, Appl. Sci., vol. 77, no. 3–4, pp. 186–192, 2023, doi: 10.2478/prolas-2023-0026.

[10] A. D. Mori, A. Karali, E. Daskalakis, R. Hing, P. S. D. Jorge, G. Cooper, G. Blunn, "Poly- ε -Caprolactone 3D-Printed Porous Scaffold in a Femoral Condyle Defect Model Induces Early Osteo-Regeneration," pp. 1–14, 2024.

[11] J. V Sanchaniya and S. Kanukuntla, "Morphology and mechanical properties of PAN nanofiber mat," J. Phys. Conf. Ser., vol. 2423, no. 1, p. 012018, 2023, doi: 10.1088/1742-6596/2423/1/012018.

[12] J. V. Sanchaniya, S.-P. Kanukuntla, S. Simon, and A. Gerina-Ancane, "Analysis of mechanical properties of composite nanofibers constructed on rotating drum and collector plate," 21st Int. Sci. Conf. Eng. Rural Dev. Proc., vol. 21, pp. 737–744, 2022, doi: 10.22616/erdev.2022.21.tf227.

[13] S. Gao, G. Tang, D. Hua, R. Xiong, J. Han, S. Jiang, Q. Zhang, C. Huang, "Stimuli-responsive bio-based polymeric systems and their applications," J. Mater. Chem. B, vol. 7, no. 5, pp. 709–729, 2019, doi: 10.1039/c8tb02491j.

[14] J. V. Sanchaniya, I. Lasenko, V. Gobins, and A. Kobeissi, "A Finite Element Method for Determining the Mechanical Properties of Electrospun Nanofibrous Mats," Polym., vol. 16, no. 6, p. 852, 2024, doi: 10.3390/polym16060852.

[15] J.V. Sanchaniya, I. Lasenko, V. Vijayan, H. Smogor, V. Gobins, A. Kobeissi, D. Goljandin, "A Novel Method to Enhance the Mechanical Properties of Polyacrylonitrile Nanofiber Mats: An Experimental and Numerical Investigation," Polymers (Basel)., vol. 16, no. 7, p. 992, Apr. 2024, doi: 10.3390/polym16070992.

[16] R. Skvorčinskienė, N. Striūgas, R. Navakas, R. Paulauskas, K. Zakarauskas, and L. Vorotinskienė, "Thermal Analysis of Waste Fishing Nets for Polymer Recovery," Waste and Biomass Valorization, vol. 10, no. 12, pp. 3735–3744, 2019, doi: 10.1007/s12649-019-00803-w.

[17] C. Wilcox, N. J. Mallos, G. H. Leonard, A. Rodriguez, and B. D. Hardesty, "Using expert elicitation to estimate the impacts of plastic pollution on marine wildlife," Mar. Policy, vol. 65, pp. 107–114, 2016, doi: 10.1016/j.marpol.2015.10.014.

[18] K. J. Parton, T. S. Galloway, and B. J. Godley, "Global review of shark and ray entanglement in anthropogenic marine debris," Endanger. Species Res., vol. 39, pp. 173–190, 2019, doi: 10.3354/esr00964.

[19] B. H. Hogan, "Net gains in aquaculture net technology," no. June, pp. 5–9, 2020.

[20] B. Qiu, M. Wang, W. Yu, S. Li, W. Zhang, S. Wang, J. Shi, "Environmentally Friendly and Broad – Spectrum Antibacterial Poly (hexamethylene guanidine)– Modified Polypropylene and," 2023.

[21] T. Sato and M. Shishido, "Mechanical and structural properties for recycled thermoplastics from waste fishing ropes," J. Mater. Cycles Waste Manag., vol. 22, no. 5, pp. 1682–1689, 2020, doi: 10.1007/s10163-020-01062-x.

[22] R. Juan, C. Domínguez, N. Robledo, B. Paredes, S. Galera, and R. A. García-Muñoz, "Challenges and opportunities for recycled polyethylene fishing nets: Towards a circular economy," Polymers (Basel)., vol. 13, no. 18, pp. 1–15, 2021, doi: 10.3390/polym13183155.

[23] A. Kozioł, K. G. Paso, and S. Kuciel, "Properties and Recyclability of Abandoned Fishing Net-Based Plastic Debris," Catalysts, vol. 12, no. 9, 2022, doi: 10.3390/catal12090948.

[24] R. Behaviors and A. L. Composites, "Rui Gou," Eff. Differ. Polypropyl. Ammonium Lignosulfonate Contents Cryst. Behav. Rheol. Behav. Mech. Prop. Ethyl. Propyl. Diene Monomer/ Polypropylene/ Ammonium, vol. 14, no. 1, pp. 2079–2096, 2019.

[25] W. Yu, F. Yang, L. Wang, Y. Liu, and J. Shi, "Starch-Based Fishing Composite Fiber and Its Degradation Behavior," Int. J. Polym. Sci., vol. 2020, 2020, doi: 10.1155/2020/9209108.

[26] M. Hyvärinen, R. Jabeen, and T. Kärki, "The modelling of extrusion processes for polymers-A review," Polymers (Basel)., vol. 12, no. 6, 2020, doi: 10.3390/polym12061306.

[27] M. Berihuete-Azorín, O. Lozovskaya, M. Herrero-Otal, and R. Piqué I Huerta, "Fishing Nets and String at the Final Mesolithic and Early Neolithic Site of Zamostje 2, Sergiev Posad (Russia)," Open Archaeol., vol. 9, no. 1, 2023, doi: 10.1515/opar-2022-0283.

[28] D. C. Chen, D. F. Chen, S. M. Huang, and W. J. Shyr, "The Investigation of Key Factors in Polypropylene Extrusion Molding Production Quality," Appl. Sci., vol. 12, no. 10, 2022, doi: 10.3390/app12105122.

[29] L. Yang, S. Li, Y. Li, M. Yang, and Q. Yuan, "Experimental Investigations for Optimizing the Extrusion Parameters on FDM PLA Printed Parts," J. Mater. Eng. Perform., vol. 28, no. 1, pp. 169–182, 2019, doi: 10.1007/s11665-018-3784-x.

[30] M. Ramesh, L. Rajeshkumar, and D. Balaji, "Influence of Process Parameters on the Properties of Additively Manufactured Fiber-Reinforced Polymer Composite Materials: A Review," J. Mater. Eng. Perform., vol. 30, no. 7, pp. 4792–4807, 2021, doi: 10.1007/s11665-021-05832-y.

[31] Y. Peng, M. Musah, B. Via, and X. Wang, "Calcium carbonate particles filled homopolymer polypropylene at different loading levels: Mechanical properties characterization and materials failure analysis," J. Compos. Sci., vol. 5, no. 11, 2021, doi: 10.3390/jcs5110302.

[32] Y. Jing, X. Nai, L. Dang, D. Zhu, Y. Wang, Y. Dong, W. Li, "Reinforcing polypropylene with calcium carbonate of different morphologies and polymorphs," Sci. Eng. Compos. Mater., vol. 25, no. 4, pp. 745–751, 2018, doi: 10.1515/secm-2015-0307.

[33] T. Thenepalli, A. Y. Jun, C. Han, C. Ramakrishna, and J. W. Ahn, "A strategy of precipitated calcium carbonate (CaCO3) fillers for enhancing the mechanical properties of polypropylene polymers," Korean J. Chem. Eng., vol. 32, no. 6, pp. 1009–1022, 2015, doi: 10.1007/s11814-015-0057-3.

[34] N. S. Yousef, "Statistical Study on Additives Used to Improve Mechanical Properties of Polypropylene," Polymers (Basel)., vol. 14, no. 1, 2022, doi: 10.3390/polym14010179.

[35] J. R. Keaton, "Young's Modulus BT - Encyclopedia of Engineering Geology," P. T. Bobrowsky and B. Marker, Eds. Cham: Springer International Publishing, 2018, pp. 955–956. doi: 10.1007/978-3-319-73568-9_298.

[36] K. Yamamoto, A. Takasaki, and N. Hosoya, "Assessment of Dynamic Young's Modulus and Damping Ratio of Bamboo Fiber Reinforced Polymer Composites using Shock Wave BT - Advances in Mechanism and Machine Science," 2019, pp. 4217–4226.

[37] H.-N. T. Pham and V.-T. Nguyen, "Effect of calcium carbonate on the mechanical properties of polyethylene terephthalate/polypropylene blends with styrene-ethylene/butylene-styrene," J. Mech. Sci. Technol., vol. 34, no. 10, pp. 3925–3930, 2020, doi: 10.1007/s12206-020-2201-1.

[38] P. Castejón, M. Antunes, and D. Arencón, "Development of inorganic particle-filled polypropylene/high density polyethylene membranes via multilayer co-extrusion and stretching," Polymers (Basel)., vol. 13, no. 2, pp. 1–16, 2021, doi: 10.3390/polym13020306.

[39] J. Z. Liang, C. Y. Tang, R. K. Y. Li, and T. T. Wong, "Mechanical properties of polypropylene/CaCC3 composites," Met. Mater., vol. 4, no. 4, pp. 616–619, 1998, doi: 10.1007/BF03026368.

[40] S. Chen, X. Wang, X. Ma, and K. Wang, "Morphology and properties of polypropylene/nano-CaCO3 composites prepared by supercritical carbon dioxide-assisted extrusion," J. Mater. Sci., vol. 51, no. 2, pp. 708–718, 2016, doi: 10.1007/s10853-015-9272-x.

[41] F. Ke, X. Jiang, H. Xu, J. Ji, and Y. Su, "Ternary nano-CaCO 3/poly(ethylene terephthalate) fiber/polypropylene composites: Increased impact strength and reinforcing mechanism," Compos. Sci. Technol., vol. 72, no. 5, pp. 574–579, 2012, doi: 10.1016/j.compscitech.2012.01.001.

[42] J.-I. Weon and H.-J. Sue, "Mechanical properties of talc- and CaCO3-reinforced high-crystallinity polypropylene composites," J. Mater. Sci., vol. 41, no. 8, pp. 2291–2300, 2006, doi: 10.1007/s10853-006-7171-x.

[43] J. P. Duarte, C. E. M. Guilherme, A. H. M. F. T. da Silva, A. C. Mendonça, and F. Tempel Stumpf, "Lifetime prediction of aramid yarns applied to offshore mooring due to purely hydrolytic degradation," Polym. Polym. Compos., vol. 27, no. 8, pp. 518–524, 2019, doi: 10.1177/0967391119851386.

[44] J. K. Edzwald and J. Haarhoff, "Seawater pretreatment for reverse osmosis: Chemistry, contaminants, and coagulation," Water Res., vol. 45, no. 17, pp. 5428–5440, 2011, doi: 10.1016/j.watres.2011.08.014.

[45] H. Xiao, S. Liu, D. Wang, and Y. Chen, "Abrasion–Corrosion Behaviors of Steel–Steel Contact in Seawater Containing Abrasive Particles," Tribol. Trans., vol. 61, no. 1, pp. 12–18, Jan. 2018, doi: 10.1080/10402004.2016.1268227.

[46] G. Han, X. Tao, X. Li, W. Jiang, and W. Zuo, "Study of the Mechanical Properties of Ultra-High Molecular Weight Polyethylene Fiber Rope," J. Eng. Fiber. Fabr., vol. 11, no. 1, p. 155892501601100100, Mar. 2016, doi: 10.1177/155892501601100103.

[47] R. Neppalli, C. Marega, A. Marigo, M.P. Bajgai, H.Y. Kim, S.S. Ray, V. Causin, "Electrospun nylon fibers for the improvement of mechanical properties and for the control of degradation behavior of poly(lactide)-based composites," J. Mater. Res., vol. 27, no. 10, pp. 1399–1409, 2012, doi: 10.1557/jmr.2012.70.

[48] M. Spoerk, J. Gonzalez-Gutierrez, C. Lichal, H. Cajner, G.R. Berger, S. Schuschnigg, L. Cardon, C. Holzer, "Optimisation of the adhesion of polypropylene-based materials during extrusion-based additive manufacturing," Polymers (Basel)., vol. 10, no. 5, 2018, doi: 10.3390/polym10050490.

[49] Abhijeet Gujrati, "Understanding Nanoscale Surface Roughness and its Effect on Macroscale Adhesion," Master Thesis, vol. 27, p. i, 2020.

[50] S. Budhe, A. Ghumatkar, N. Birajdar, and M. D. Banea, "Effect of surface roughness using different adherend materials on the adhesive bond strength," Appl. Adhes. Sci., vol. 3, no. 1, pp. 0–9, 2015, doi: 10.1186/s40563-015-0050-4.

[51] M. D. Roussel, A. R. Guy, L. G. Shaw, and J. E. Cara, "The use of calcium carbonate in polyolefins offers significant improvement in productivity," TAPPI Eur. PLACE Conf., vol. 1, pp. 225–236, 2005.